

Ymer Acts as a Multifunctional Regulator in Nuclear Factor- κ B and Fas Signaling Pathways

Tadasuke Tsukiyama,¹ Mayuko Matsuda-Tsukiyama,¹ Miyuki Bohgaki,¹ Sayuri Terai,¹ Shinya Tanaka,² and Shigetsugu Hatakeyama¹

Departments of ¹Biochemistry and ²Pathology, Hokkaido University Graduate School of Medicine, Sapporo, Hokkaido, Japan

The nuclear factor (NF)- κ B family of transcription factors regulates diverse cellular functions, including inflammation, oncogenesis and apoptosis. It was reported that A20 plays a critical role in the termination of NF- κ B signaling after activation. Previously, we showed that Ymer interacts and collaborates with A20, followed by degradation of receptor-interacting protein (RIP) and attenuation of NF- κ B signaling. Here we show the function of Ymer in regulation of several signaling pathways including NF- κ B on the basis of results obtained by using Ymer transgenic (*Ymer Tg*) mice. *Ymer Tg* mice exhibited impaired immune responses, including NF- κ B and mitogen-activated protein kinase (MAPK) activation, cell proliferation and cytokine production, to tumor necrosis factor (TNF)- α , polyI:C or lipopolysaccharide (LPS) stimulation. *Ymer Tg* mice were more resistant to LPS-induced septic shock than wild-type mice. Transgene of *Ymer* inhibited the onset of glomerulonephritis in *lpr/lpr* mice as an autoimmune disease model. In contrast to the inflammatory immune response to LPS, Fas-mediated cell death was strongly induced in liver cells of *Ymer Tg* mice in which Ymer is abundantly expressed. These findings suggest that Ymer acts as a regulator downstream of several receptors and that Ymer functions as a positive or negative regulator in a signaling pathway-dependent manner.

Online address: <http://www.molmed.org>

doi: 10.2119/molmed.2011.00435

INTRODUCTION

Nuclear factor (NF)- κ B is a ubiquitously expressed transcription factor that induces the expression of target genes and regulates diverse cellular functions including inflammation, immunity, cell growth and apoptosis in response to various stimuli (1). NF- κ B is an important molecule downstream of the tumor necrosis factor receptor (TNFR) and Toll-like receptor (TLR). Tumor necrosis factor (TNF)- α stimulation results in recruitment of receptor-interacting protein (RIP) to the intracellular region of TNFR, and then RIP undergoes lysine (K) 63-linked polyubiquitination by ubiquitin-conjugating enzyme 13 (Ubc13)/ubiquitin-conjugating

enzyme E2 variant 1 (Uev1) A and TNFR-associated factor 2 (TRAF2) as E2 and E3, respectively. The K63-linked polyubiquitin chain on RIP activates transforming growth factor (TGF)- β -associated kinase (TAK)/TAK1 binding protein (TAB) kinase complex. Activated TAK/TAB complex phosphorylates and activates the I κ B kinase (IKK) complex, which consists of IKK α , IKK β and IKK γ /Nemo. Activated IKK β phosphorylates I κ B, and then phosphorylated I κ B is recognized and ubiquitinated by a ubiquitin ligase complex, SCF^{Fbw1} (Skp1-Cul1-F-box complex containing Fbw1), followed by degradation of I κ B via a proteasome-dependent pathway and activation of NF- κ B (2,3).

However, termination of NF- κ B activation is usually required after transient activation, because sustained activation of NF- κ B causes excess inflammatory cytokine secretion, by which systemic and lethal shock such as a cytokine storm may be induced. A unique intracellular enzyme, A20, is induced by NF- κ B activation and plays an important role in attenuating NF- κ B signaling (4). A20 hydrolyzes the K63-linked polyubiquitin chain on RIP and then conjugates the K48-linked polyubiquitin chain. K48-linked polyubiquitinated RIP is degraded by proteasome, resulting in termination of the NF- κ B signal (5). Taken together, the results indicate that induction of A20 after activation of NF- κ B functions as a negative feedback loop to return to a resting state. It was reported that A20 is a unique and key molecule that negatively regulates NF- κ B signaling, as indicated by experiments using A20-disrupted mice, in which drastic systemic inflammation occurs a few weeks after birth followed by early death (4). We have shown that Ymer is a novel A20-interacting protein by yeast two-

Address correspondence to Shigetsugu Hatakeyama, Department of Biochemistry, Hokkaido University Graduate School of Medicine, Kita15, Nishi7, Kita-ku, Sapporo 060-8638, Japan. Phone: +81-11-706-5047; Fax: +81-11-706-5169; E-mail: hatas@med.hokudai.ac.jp. Submitted November 8, 2011; Accepted for publication February 3, 2012; Epub (www.molmed.org) ahead of print February 6, 2012.

hybrid screening (6). Ymer is a cytoplasmic protein containing a coiled-coil region and two motifs interacting with ubiquitin (MIU) domains. Overexpression of Ymer diminishes NF- κ B signaling, whereas knockdown of endogenous Ymer upregulates NF- κ B signaling, suggesting that Ymer functions as a negative regulator for NF- κ B signaling.

To examine the physiological function of Ymer in NF- κ B signaling, we generated CAG promoter-driven Ymer transgenic (*Ymer Tg*) mice. *Ymer Tg* mice were viable and fertile, but they exhibited impaired immunoreactions and apoptosis in response to TNF α and lipopolysaccharide (LPS) stimulation *in vitro* and *in vivo*. In contrast to TNF α and LPS stimulation, Fas-mediated apoptosis of hepatocytes was greatly enhanced in Ymer-expressing *Tg* mice. These observations suggest that Ymer functions as a receptor-dependent multidirectional regulator that suppresses TNFR or TLR3/4-dependent NF- κ B signaling but enhances Fas-dependent signaling.

MATERIALS AND METHODS

Transgenic Mice

The *Bam*HI/*Xho*I fragment of FLAG-tagged human Ymer cDNA from pCR-FLAG-Ymer was ligated into the *Bgl*III/*Xho*I sites of pCAGI-puro, and then the *Kpn*I/*Not*I fragment from it was transferred into the *Kpn*I/*Not*I sites of pCAGGS-p7 (7). The *Sall*/*Bam*HI fragment (3.6 kb) from this plasmid was microinjected into the pronuclei of fertilized mouse zygotes derived from BDF1 (C57BL/6 \times DBA) \times BDF1 crosses. The injected zygotes were implanted into the uterus of pseudo-pregnant ICR mice, and the progeny were screened by polymerase chain reaction (PCR) with human Ymer-specific internal primers: forward, 5'-TTTTT AATGT TTGTA ATGAA AACCT TTATG-3'; reverse, 5'-GGTAT GGCTG AAGTC AGCAT CGACC AGTCC-3'. Transgenic mouse lines were propagated by sequential backcrossing to C57BL/6 mice. The F4-5 mice were used for the experiments at

6–8 wks of age. Southern blot analysis was performed to confirm genetic integration of the transgene with the *Xho*I/*Not*I fragment of the transgenic construct, which contains the full length of human Ymer cDNA. All animal experiments were carried out in accordance with the National Institutes of Health *Guide for the Care and Use of Laboratory Animals* (8) and were approved by the animal care and use committee of Hokkaido University.

Cell Culture, Reagents, Transfection and Reporter Assay

Mouse thymocytes, splenocytes or macrophages were cultured in RPMI 1640 (Sigma, St. Louis, MO, USA) supplemented with 10% fetal bovine serum (Invitrogen, Carlsbad, CA, USA). Mouse embryonic fibroblasts (MEFs) were cultured in Dulbecco's modified Eagle's medium supplemented with 10% fetal bovine serum (Invitrogen). All of these primary cells were incubated under an atmosphere of 5% CO₂ at 37°C. Luciferase reporter assay for NF- κ B activities was carried out using the NAT reporter system (9). Briefly, wild-type (WT) and *Ymer Tg* MEFs (1×10^5 cells) were seeded into 24-well plates and were transfected with NAT-EGFP:Luc2 reporter plasmids (100 ng/well) and *Renilla* reporter gene plasmids (2 ng/well) with FuGENE HD Transfection Reagent (Roche, Mannheim, Germany). Twelve hours after transfection, cells were further stimulated for 12 h with TNF α (20 ng/mL; Sigma). The cells were then harvested and lysed with lysis buffer (100 μ L). Luciferase activities were measured using 20 μ L lysate and 100 μ L luciferase assay substrates (Promega, Madison, WI, USA). The luminescence was quantified with a luminometer (Promega).

Flow Cytometry

Single splenocyte suspensions were stained with phycoerythrin-Cy5 (PE-Cy5)-conjugated anti-B220 (RA3-6B2; eBioscience, San Diego, CA, USA), fluorescein isothiocyanate (FITC)-conjugated

anti-Mac-1a (M1/70; eBioscience) and PE-conjugated anti-T-cell receptor β (anti-TCR β) (H57-597; eBioscience) antibodies (Abs). Purified macrophages or thymocytes were stained with Abs against PE-conjugated anti-TNFR1 (55R-286; BioLegend, San Diego, CA, USA), anti-TLR4 (MTS510; eBioscience) or anti-Fas (Jo2; BD Pharmingen, San Jose, CA, USA). All analyses were performed with a FACSCalibur flowcytometer and CellQuest software (Becton Dickinson, San Jose, CA, USA).

In Vitro or *In Vivo* Splenocyte Proliferation in Response to LPS or TNF α

Isolated splenocytes were stimulated with LPS (100 ng/mL) from *Escherichia coli* 055:B5 (Sigma), and cell proliferation was measured with CellTiter 96 Aqueous One Solution Reagent (Promega) and MULTISKAN JX (ThermoFisher, Waltham, MA, USA) at the indicated day according to the manufacturer's protocol. Splenocyte proliferation *in vivo* was assessed by intraperitoneal injection with TNF α (50 μ g/kg; Sigma) or LPS (100 μ g/kg) in 0.9% saline. Three days after injection, TNF α or LPS-injected spleens were isolated and analyzed with a flowcytometer. Survival study against endotoxin shock was performed by intraperitoneal injection of LPS (50 mg/kg) in 0.9% saline.

Macrophage Purification and Stimulation

Three days after intraperitoneal injection of 3% thioglycollate, peritoneal macrophages were isolated from WT and *Ymer Tg* mice and then macrophages were seeded into a six-well plate (1×10^6 cells/well). One hour after culture, the plates with seeded cells were washed with phosphate-buffered saline (PBS) three times to remove cells other than macrophages. The purity of isolated macrophages was confirmed by flowcytometric analysis with anti-Mac-1 monoclonal antibody (Supplementary Figure 3). The percentages of isolated macrophages were >85%. Purified

macrophages were stimulated with LPS (1 $\mu\text{g}/\text{mL}$; Sigma).

RNA Isolation, Reverse Transcription-PCR and Quantitative Real-Time PCR

Cells and tissues stimulated with LPS or polyI:C (high molecular weight [HMW], 50 $\mu\text{g}/\text{mL}$; Invitrogen) were homogenized in Isogen reagent (Nippon Gene, Tokyo, Japan) according to the manufacturer's protocol. Reverse transcription-polymerase chain reactions (RT-PCRs) were performed in a total volume of 20 μL containing total RNA (400 ng) at 50°C for 30 min using ReverTra-Plus (Toyobo, Osaka, Japan). PCR was carried out as follows: 25–28 cycles of denaturalization at 94°C for 20 s, annealing at 60°C for 20 s and extension at 72°C for 30 s. The primer sequences were obtained from the PrimerBank database (<http://pga.mgh.harvard.edu/primerbank>) as follows: *Ppia*, forward: 5'-GAGCT GTTG CAGAC AAAGT TC-3'; *Ppia*, reverse: 5'-CCCTG GCACA TGAAT CCTGG-3'; *IL-1 β* , forward: 5'-GACAG TGATG AGAAT GACCT-3'; *IL-1 β* , reverse: 5'-CTAAT GGGAA CGTCA CACAC C-3'; *IL-6*, forward: 5'-GAGAG GAGAC TTCAC AGAGG ATAC-3'; *IL-6*, reverse: 5'-GTACT CCAGA AGACC AGAGG-3'; *TNF α* , forward: 5'-GACGT GGAAC TGGCA GAAGA G-3'; *TNF α* , reverse: 5'-TTGGT GGTG GTGAG TGTGA G-3'; interferon (*IFN*)- α , forward: 5'-CTTCC ACAGG ATCAC TGTGT ACCT-3'; *IFN*- α , reverse: 5'-TTCTG CTCTG ACCAC CTCCC-3'; inducible nitric oxide synthase (*iNOS*), forward: 5'-GTTCT CAGCC CAACA ATACA AGA-3'; and *iNOS*, reverse: 5'-GTGGA CGGGT CGATG TCAC-3'. Quantitative real-time PCRs and analyses were performed with Power SYBR Green PCR Master Mix (Applied Biosystems, Foster City, CA, USA) using a StepOne Real-Time PCR System (Applied Biosystems).

Quantification of Secreted IL-6 by Enzyme-Linked Immunosorbent Assay

Sera from the mice treated with LPS or culture supernatant of LPS-stimulated

macrophages were used for mouse IL-6 enzyme-linked immunosorbent assay (ELISA) Ready-Set-Go (eBioscience) and MULTISKAN JX according to the manufacturer's protocol.

Fas-Induced Apoptosis and Histological Analysis

Apoptosis of thymocytes was induced with anti-Fas Ab (Jo2, 10 $\mu\text{g}/\text{mL}$). Briefly, thymocytes (1×10^7 cells) were stimulated with anti-Fas Ab for 5 min at 37°C, washed and then incubated for the indicated periods. Apoptosis of hepatocytes was induced by intraperitoneal injection of anti-Fas Ab (20 $\mu\text{g}/\text{mice}$). Four or two hours after injection, livers were isolated from two mice of each genotype and then used for hematoxylin-eosin (HE) staining or for immunoblot analysis, respectively. Livers freshly isolated from mice were fixed overnight in 10% formalin/PBS, dehydrated in methanol and embedded in paraffin. Serial sections (10 μm) were stained with HE and analyzed using BX51 and DP71 microscopic systems (Olympus, Tokyo, Japan).

Immunoblot Analysis

Cells or tissues isolated from mice were lysed with a solution containing 50 mmol/L Tris-HCl (pH 7.6), 300 mmol/L NaCl, 0.5% Triton X-100, aprotinin (10 $\mu\text{g}/\text{mL}$), leupeptin (10 $\mu\text{g}/\text{mL}$), 10 mmol/L iodoacetamide, 1 mmol/L phenylmethylsulfonyl fluoride (PMSF), 0.4 mmol/L Na_3VO_4 , 0.4 mmol/L EDTA, 10 mmol/L NaF and 10 mmol/L sodium pyrophosphate. The lysates were incubated on ice for 20 min and then centrifuged at 16,000g for 20 min at 4°C. After determination of protein concentrations with the Bradford assay (Bio-Rad Laboratories, Hercules, CA, USA), cell lysates (20 μg) were subjected to sodium dodecyl sulfate-polyacrylamide gel electrophoresis on 8% or 10% gel, and separated proteins were transferred to an Immobilon-P membrane (Millipore, Bedford, MA, USA). The membranes were probed with Abs for poly(ADP-ribose) polymerase (PARP) (9532; Cell Signaling

Technology [CST], Danvers, MA, USA), phospho-IKK (2681; CST), IKK (2684; CST), phospho-JNK (c-Jun N-terminal kinase) (9251; CST), JNK (9252; CST), phospho-extracellular signal-regulated kinase (phospho-ERK) (9101; CST), ERK (9102; CST), phospho-p38 (9211; CST), p38 (9212; CST), FLAG (M5; Sigma), Ymer (6), α/β -tubulin (2148; CST), HSP70 (heat shock protein 70) (7; BD Pharmingen) and GAPDH (glyceraldehyde-3-phosphate dehydrogenase) (6C5; Applied Biosystems). Immune complexes were detected with horseradish peroxidase-conjugated Abs to mouse or rabbit IgG (Promega) and enhanced chemiluminescence (GE Healthcare Bioscience, Piscataway, NJ, USA) or Immobilon Western reagents (Millipore).

Quantification of Urinary Protein

*Ymer*⁵⁴⁵ *Tg* mice, which are backcrossed with C57BL/6 mice five times, were further crossed with B6-*lpr* mice to obtain B6-*lpr*;*Ymer Tg*⁵⁴⁵ hybrid mice. Urinary protein from B6-*lpr*;*Ymer Tg*⁵⁴⁵ hybrid mice was measured every 2 wks using an albustick (Siemens Healthcare Diagnostics K.K., Tokyo, Japan) during 4–18 wks of age.

Histological Analysis of Glomerulonephritis

Tissues were dissected out at 7–8 months of age and fixed in 10% formalin for 24 h at 4°C. Paraffin sections (4 μm) were stained with the periodic acid Schiff (PAS) procedure and evaluated by light microscopy. The frequencies of inflammatory glomeruli, which exhibit the proliferation of mesangium cells (containing more than four cells in a mesangial region), were scored by observation from 20 glomeruli that were randomly selected in each kidney.

Statistical Analysis

The Student *t* test (Figures 1A, 2C, 3C, E and Supplementary Figure 4), Welch *t* test (Figures 1C, 2D, 4C) and Kaplan-Meier test (Figures 2B and 5A and Supplementary Figure 1D) were used to measure differences among samples.

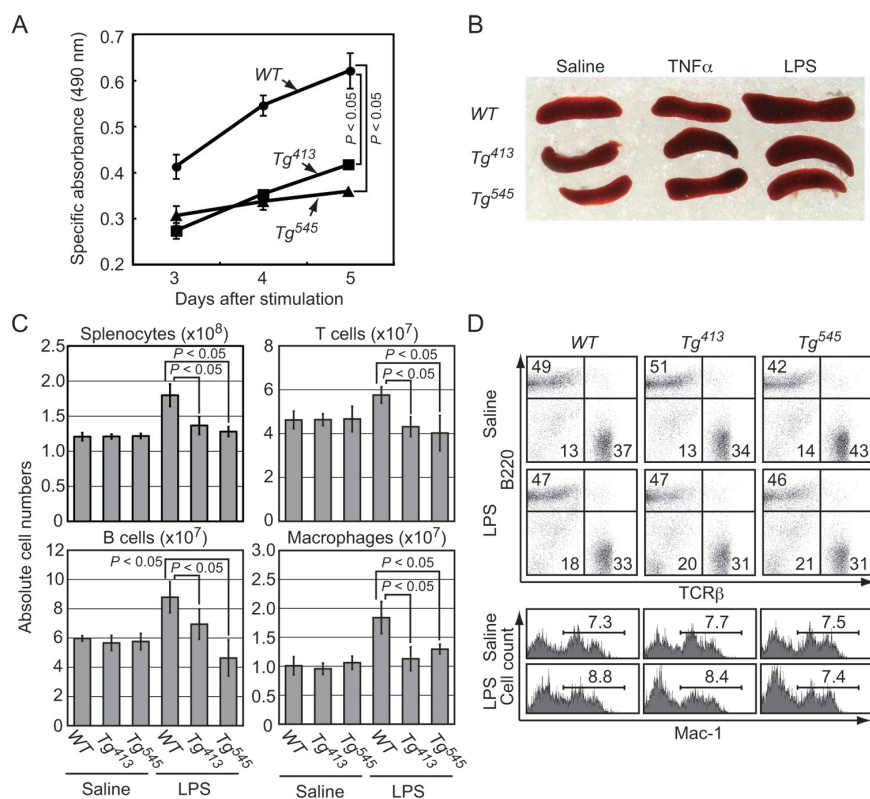


Figure 1. Impaired immune response of *Ymer Tg* mice to TNF α and LPS stimulations. (A) Splenocytes (1×10^6) isolated from WT and *Ymer Tg* mice were stimulated with LPS (100 ng/mL), and cell proliferation was measured by an MTS assay. (B) Four days after injection with TNF α (50 μ g/kg) or LPS (100 μ g/kg), spleens were dissected out from WT and *Ymer Tg* mice. (C) Cell numbers in LPS-stimulated spleen in *Ymer Tg* mice. Cell numbers of splenocytes in (B) were counted (saline-treated WT, n = 4; saline-treated Tg⁴¹³, n = 4; saline-treated Tg⁵⁴⁵, n = 3; LPS-treated WT, n = 5; LPS-treated Tg⁴¹³, n = 3; LPS-treated Tg⁵⁴⁵, n = 4). (D) Flowcytometric analysis of LPS-treated splenocytes in *Ymer Tg* mice. Splenocytes in (B) were analyzed by flowcytometry using anti-B220, anti-TCR β and anti-Mac-1 Abs. Percentages of each population are indicated in the panels.

All supplementary materials are available online at www.molmed.org.

RESULTS

Impaired Response of Splenocytes to TNF α and LPS Stimulations in *Ymer Tg* Mice

To examine the physiological function of Ymer, we established two strains of CAG promoter-driven *Ymer Tg* mice (*Ymer Tg*⁴¹³ and *Ymer Tg*⁵⁴⁵) (Supplementary Figure 1). Immunoblot analysis with anti-Ymer and anti-FLAG Abs showed that the two strains have slightly different expression patterns. Tg⁵⁴⁵ mice highly ex-

pressed exogenous Ymer in the liver and macrophages, whereas Tg⁴¹³ mice had low expression levels of exogenous Ymer in the liver and macrophages. In contrast, Tg⁴¹³ mice highly expressed exogenous Ymer in MEFs (Figures 3A, 5D and Supplementary Figure 1).

We then examined the immune responses of splenocytes isolated from WT and *Ymer Tg* mice to LPS stimulation. Although *Ymer Tg* mice were healthy and displayed a normal lifespan and development of immune cells, including T cells, B cells and macrophages, splenocytes isolated from *Ymer Tg* mice exhibited impaired proliferation after LPS stimulation

compared with WT splenocytes (Figure 1 and Supplementary Figures 1D, 2). Splenomegaly and increase in total splenocyte number were induced in WT mice by *in vivo* LPS administration (100 μ g/kg), whereas splenomegaly and increase in total splenocyte number were inhibited in both lines of *Ymer Tg* mice (Figures 1B, C). Flowcytometric analysis showed that proliferation of splenic T-cell, B-cell and macrophage subsets in *Ymer Tg* mice was inhibited after injection of LPS, suggesting that excess expression of Ymer attenuates immune response via TLR4 to LPS *in vivo* (see Figure 1C). However, the ratio of cell number of each subset was not changed (Figure 1D).

Resistance to LPS-Induced Septic Shock in *Ymer Tg* Mice

It was reported that LPS or TNF α induces activation of caspase 3 in hepatocytes, followed by cleavage of poly(ADP-ribose) polymerase (PARP) and apoptosis (10,11). To examine whether cleavage of PARP after administration of LPS or TNF α is affected by overexpression of Ymer, immunoblot analysis with anti-PARP Abs was performed using *Ymer Tg* mice. The cleavage product of PARP at 50 kDa, which has been reported as evidence of necrotic cell death (12), was observed in WT mice with LPS or TNF α treatment, but cleavage products were not observed in either line of *Ymer Tg* mice (Figure 2A). These findings suggest that overexpression of Ymer causes decrease in the NF- κ B signal via TLR4 or TNFR in hepatocytes as well as splenocytes. To confirm activation of NF- κ B signaling in hepatocytes stimulated with LPS or TNF α , we examined the expression level of RIP and activation of IKK α / β in *Ymer Tg* mice. Stimulation with LPS or TNF α caused a decrease in expression level of RIP and phosphorylation of IKK α / β in hepatocytes of WT mice, whereas stimulation with LPS or TNF α did not cause a decrease in expression level of RIP and phosphorylation of IKK α / β in hepatocytes of *Ymer Tg* mice (see Figure 2A). It was reported that the expression level of RIP and phosphorylation of IKK α / β after

NF- κ B activation were inhibited by negative feedback machinery including A20 (4). Taken together, because NF- κ B activation is inhibited in *Ymer Tg* mice, negative feedback to downregulate RIP may be suppressed. These findings suggest that overexpression of Ymer protein in splenocytes and hepatocytes causes impaired response via TNFR and TLR4 and that negative feedback after NF- κ B activation is inhibited in *Ymer Tg* mice.

In addition to low-dose stimulation with LPS (50 μ g/kg i.p.) (see Figure 2A), we also examined viability of *Ymer Tg* mice with a high dose of LPS (50 mg/kg i.p.). Statistical analysis showed that *Ymer Tg⁵⁴⁵* mice were more resistant to LPS than WT mice (WT versus *Tg⁵¹⁴*; $P = 0.321$; WT versus *Tg⁵⁴⁵*; $P < 0.05$) (Figure 2B). These findings suggest that *Ymer Tg* mice have resistance to LPS-induced septic shock. To clarify at the molecular level why *Ymer Tg* mice are resistant to LPS, mRNA levels of LPS-induced target genes including several proinflammatory cytokines and iNOS were examined by quantitative real-time polymerase chain reaction (qRT-PCR) (13,14). The gene expressions of *IL-1 β* , *IL-6*, *TNF α* and *iNOS* were downregulated in both *Ymer Tg* lines with LPS, whereas the expression of *IFN α* was upregulated in *Ymer Tg* mice (Figure 2C). In addition, we observed a similar effect of Ymer on cytokine production in polyI:C-stimulated splenocytes, suggesting that Ymer also regulates TLR3-mediated signal transduction (15,16) (Supplementary Figure 4). ELISA was also performed to confirm the levels of IL-6 in sera from LPS-treated mice, and the results showed that secretion of IL-6 in sera with LPS stimulation was inhibited in *Ymer Tg* mice (Figure 2D). These findings suggest that cytokine production by NF- κ B activation was inhibited in *Ymer Tg* mice, and consequently LPS-induced septic shock was suppressed in *Ymer Tg* mice.

Impaired NF- κ B Response of Macrophages in *Ymer Tg* Mice

Next, to determine whether downstream molecules are affected by LPS

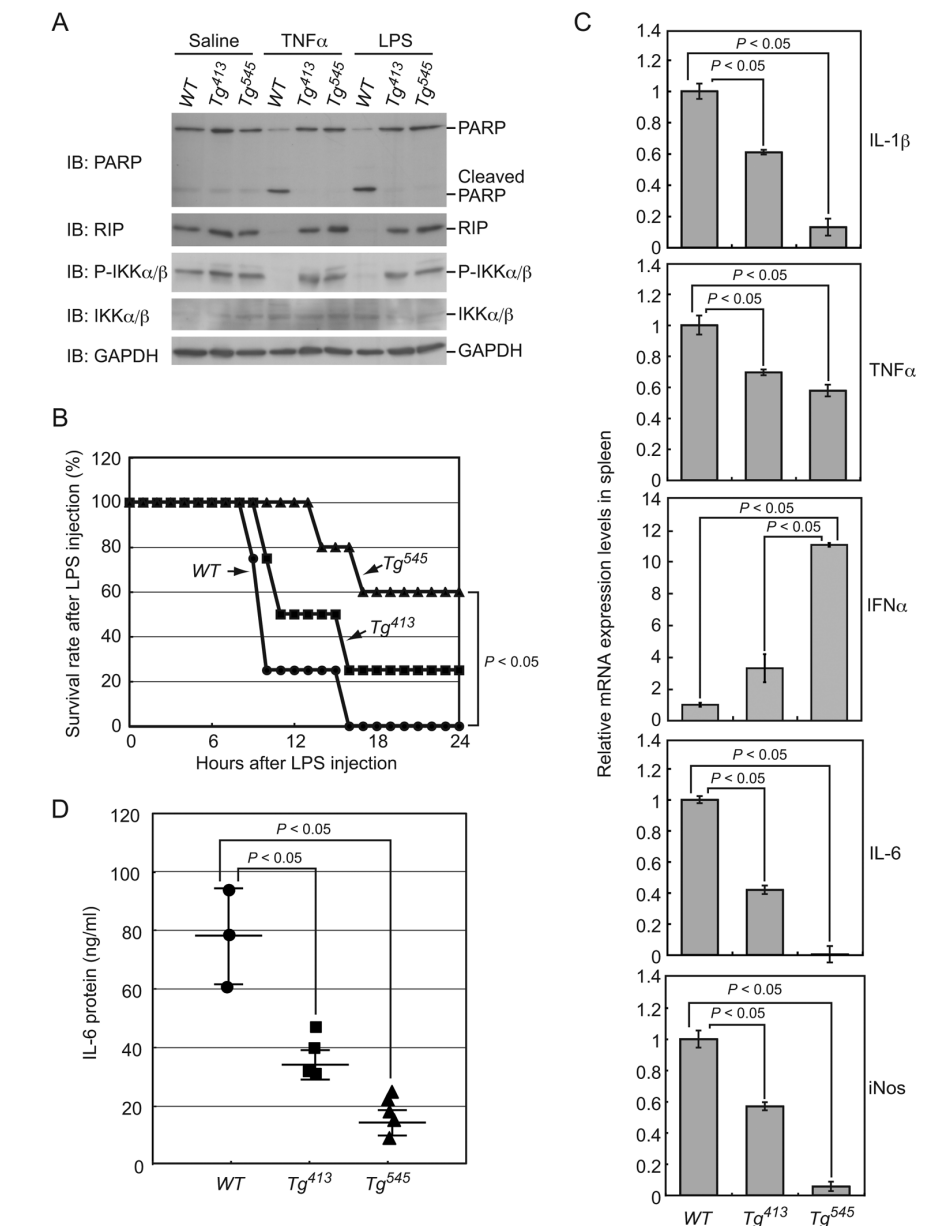


Figure 2. Resistance to septic shock in *Ymer Tg* mice. (A) Immunoblot analysis of *Ymer Tg* mice treated with TNF α or LPS. Three days after intraperitoneal injection with TNF α or LPS, cell lysates from the livers of WT and *Ymer Tg* mice were used for immunoblot analysis with Abs against PARP, RIP, IKK and P-IKK. (B) Survival study of *Ymer Tg* mice by LPS. WT and *Ymer Tg* mice were injected with LPS (50 mg/kg) and then observed for 24 h (WT, $n = 4$; *Tg⁴¹³*, $n = 4$; *Tg⁵⁴⁵*, $n = 5$). (C) Production of inflammatory cytokines in *Ymer Tg* mice. Expression levels of *IL-1 β* , *IL-6*, *TNF α* , *IFN α* and *iNOS* were measured by qRT-PCR at 4 h after LPS injection. (D) Secretion of IL-6 in sera of *Ymer Tg* mice. Four hours after LPS injection, IL-6 concentrations of sera from WT and *Ymer Tg* mice were measured by ELISA (WT, $n = 3$; *Tg⁴¹³*, $n = 4$; *Tg⁵⁴⁵*, $n = 5$).

stimulation using macrophages from *Ymer Tg* mice, immunoblot analysis was performed with Abs to signaling molecules including the IKK and mitogen-

activated protein kinase (MAPK) families. Immunoblot analysis showed that activations of p38 MAPK and JNK were attenuated in *Tg⁵⁴⁵* mice, in which exogenous

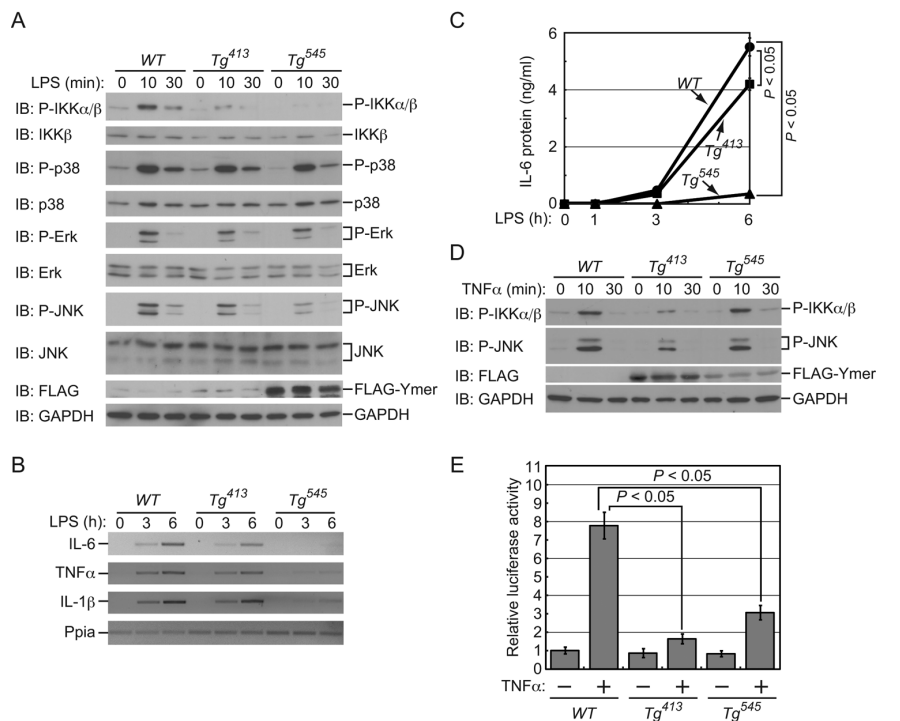


Figure 3. Impaired activation after treatment with LPS or TNF α in *Ymer Tg* mice. (A) Thioglycollate-induced peritoneal macrophages isolated from *WT* and *Ymer Tg* mice were stimulated with LPS (1 μ g/mL) for the indicated times, and the cell lysates were analyzed by immunoblotting to detect the activation of IKK and MAPK. The percentages of isolated macrophages were >85%. (B) Cytokine production in thioglycollate-induced peritoneal macrophages from *Ymer Tg* mice after treatment with LPS. mRNA expression levels of cytokines (IL-6, TNF α and IL-1 β) were analyzed by reverse transcription-polymerase chain reactions (RT-PCRs). (C) IL-6 production by thioglycollate-induced peritoneal macrophages from *Ymer Tg* mice after treatment with LPS. ELISA was performed to measure IL-6 production in the culture supernatant at the indicated times. (D) MEFs isolated from *WT* and *Ymer Tg* mice were stimulated with TNF α (10 ng/mL) for the indicated times, and the cell lysates were analyzed by immunoblotting to detect the activation of IKK and JNK. (E) NF- κ B luciferase reporter assay using MEFs from *Ymer Tg* mice. Eight hours after TNF α (10 ng/mL) stimulation, NF- κ B-dependent transcriptional activities were measured.

FLAG-Ymer is abundantly expressed (Figure 3A). Similar to MAPK signaling, IKK phosphorylation, which reflects activity of NF- κ B signaling, was inhibited in *Ymer Tg* mice compared with that in *WT* mice. Taken together, the results indicate that activation of both MAPK and NF- κ B signaling with LPS stimulation is suppressed in macrophages from *Ymer Tg* mice. To confirm suppression of NF- κ B signaling by overexpression of Ymer, we examined the expression levels of NF- κ B target genes by reverse transcription-polymerase chain reactions (RT-PCRs) and IL-6 production by ELISA using LPS-stimulated macro-

phages (Figures 3B, C). mRNA levels of several cytokines (IL-6, TNF α and IL-1 β ; Figure 3B) and the secretion of IL-6 protein in *Ymer Tg* mice, especially in *Tg⁵⁴⁵* mice, were lower than those in *WT* mice (Figure 3C). We further analyzed activation of NF- κ B signaling using MEFs derived from *Ymer Tg* mice. Activation of IKK α/β and JNK with TNF α was inhibited in MEFs from *Ymer Tg⁴¹³* mice, in which exogenous FLAG-Ymer is highly expressed, whereas activation of both IKK α/β and JNK were observed after TNF α stimulation in MEFs from *WT* and *Tg⁵⁴⁵* mice (Figure 3D). To examine NF- κ B-mediated

transcription, a luciferase reporter assay for NF- κ B signaling was performed using MEFs. The luciferase assay showed that NF- κ B-mediated transcription with TNF α was suppressed in MEFs from *Ymer Tg* mice and that overexpression of Ymer suppressed NF- κ B signaling in a dose-dependent manner (Figure 3E). These findings suggest that excess Ymer expression causes inhibition of downstream signaling and production of inflammatory cytokines.

Ymer Negatively Regulates Inflammations Induced in *lpr/lpr* Mice

We showed that Ymer inhibits inflammatory signaling including NF- κ B with several stimulations. It is well known that *lpr/lpr* mice that lack Fas expression exhibit systemic lupus erythematosus-like autoimmune disease and that the inflammatory phenotypes induced by the *lpr/lpr* genotype are different in a genetic background-dependent manner (17). To evaluate the physiological function of Ymer *in vivo*, we introduced *Ymer Tg⁵⁴⁵* transgene into *B6-lpr/lpr* mice; these mice exhibit more mild inflammation than *MRL-lpr/lpr* mice and show a slight increase in urinary protein level and glomerulonephritis in the kidney (17). *B6-lpr/lpr* mice exhibited increasing levels of proteinuria after 10 wks of age, as previously reported. However, the levels of urinary protein in *B6-lpr/lpr;Ymer Tg⁵⁴⁵* mice were almost normal and similar to those of *B6-lpr/+;Ymer Tg⁵⁴⁵* mice (Figure 4A). To confirm the inhibitory effect of Ymer on autoimmune-mediated inflammation, we performed histochemical analysis for renal inflammation using *B6-lpr/lpr;Ymer Tg⁵⁴⁵* mice. Histochemical analysis with PAS staining showed that *B6-lpr/lpr* mice caused proliferation of cells in the mesangial region of the glomerulus, in which mesangial cell proliferation as glomerulonephritis is weaker than *MRL-lpr/lpr* mice, as previously reported (17). However, mesangial cell proliferation was not observed in the kidney from *B6-lpr/lpr;Ymer Tg⁵⁴⁵* mice as well as *B6-lpr/+;Ymer Tg⁵⁴⁵* mice (Figure 4B). Quantitative analysis showed

that the frequency of mesangial proliferation in the glomerulus in *B6-lpr/lpr;Ymer Tg⁵⁴⁵* mice was significantly lower than *B6-lpr/lpr* mice (Figure 4C). These results indicated that Ymer inhibits inflammation induced in *lpr* autoimmune model mice.

Ymer Enhances Fas-Mediated Apoptosis of Hepatocytes

We previously reported that Ymer interacts with RIP and accelerates degradation of RIP, which regulates the NF- κ B signal, and others have reported that RIP functions as a downstream molecule of Fas, which regulates cell death (6,18). Although Figure 4 demonstrated that Ymer inhibits the inflammation induced in mice lacking the Fas-mediated signal, it is not clear whether Ymer affects the Fas-mediated apoptotic pathway. It was reported that anti-Fas Ab administration induces drastic apoptosis in liver cells. Therefore, to examine the effect of Ymer in the Fas-mediated apoptotic pathway, we analyzed Fas-mediated liver injury (fulminant hepatitis) with anti-Fas Ab using *Ymer Tg* mice. Surprisingly, anti-Fas Ab killed *Ymer Tg⁵⁴⁵* mice from 6 h after injection, whereas it killed both WT and *Tg⁴¹³* mice from 10 h (Figure 5A). The survival rate of *Ymer Tg⁵⁴⁵* mice was lower than that of WT and *Tg⁴¹³* mice at 24 h after anti-Fas Ab treatment, but the difference was not statistically significant (WT versus *Tg⁵⁴⁵*, $P = 0.227$). Anti-Fas Ab treatment caused hemorrhage in the liver of *Ymer Tg⁵⁴⁵* mice at 6 h after injection, but it did not cause liver hemorrhage in WT and *Tg⁴¹³* mice (Figure 5B). Histological analysis showed that anti-Fas Ab treatment induced partial apoptosis in the liver of WT and *Ymer Tg⁴¹³* mice at 4 h but that it caused massive apoptosis with hemorrhage in the liver of *Tg⁵⁴⁵* mice (Figure 5C).

To determine whether apoptosis-related proteins in *Ymer Tg⁵⁴⁵* mice are affected by anti-Fas Ab treatment, we performed immunoblot analysis with Abs against apoptosis-related proteins using lysates prepared from the liver at 2 h after anti-Fas Ab administration. Im-

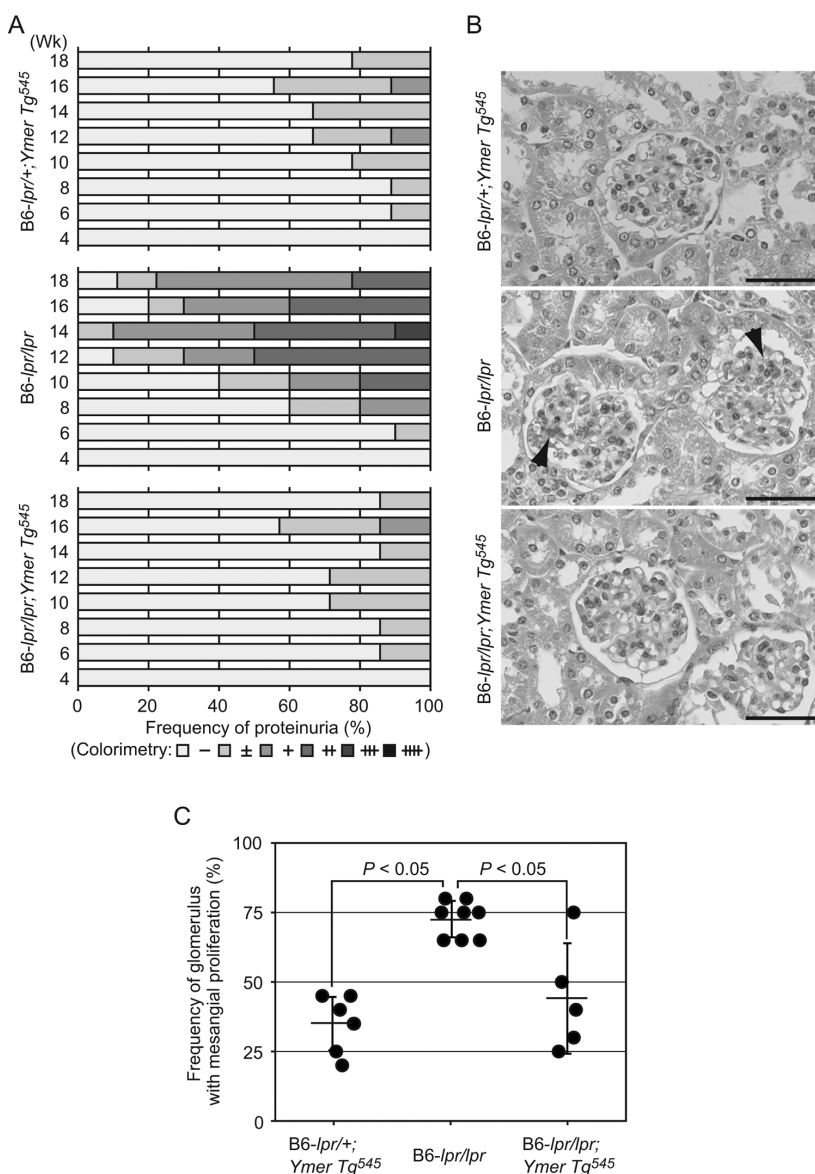


Figure 4. Ymer inhibits glomerulonephritis in *lpr/lpr* mice. (A) The levels of urinary protein in *B6-lpr/+;Ymer⁵⁴⁵*, *B6-lpr/lpr* and *B6-lpr/lpr;Ymer⁵⁴⁵* mice. Urinary proteins were measured during 4–18 wks of age (*B6-lpr/+;Ymer⁵⁴⁵*, $n = 9$; *B6-lpr/lpr*, $n = 10$; *B6-lpr/lpr;Ymer⁵⁴⁵*, $n = 7$). (B) Histochemical analysis of glomerulonephritis. Renal tissues were dissected out at 7–8 months of age and used for histochemical analysis with PAS staining. Arrows indicate the proliferation of mesangium cells in the glomerulus. Scale bars indicate 50 μ m. (C) Quantification of glomerulonephritis in *Ymer Tg* mice crossed with *lpr* mice. The frequency of inflammatory glomerulus in which cells were proliferated in the mesangial region was quantified using *B6-lpr;Ymer* hybrid mice (*B6-lpr/+;Ymer⁵⁴⁵*, $n = 7$; *B6-lpr/lpr*, $n = 8$; *B6-lpr/lpr;Ymer⁵⁴⁵*, $n = 5$). Each dot indicates the score of glomerulonephritis obtained from individual mice. The Welch t test was used to measure differences among samples.

munoblot analysis showed that exogenous FLAG-Ymer was highly expressed in the liver of *Ymer Tg⁵⁴⁵* mice (Supplementary Figure 1C), and reduction of the

intact form of PARP (116 kDa) and increase in the cleaved form of PARP (89 kDa) as apoptotic markers were observed in *Ymer Tg⁵⁴⁵* mice with anti-Fas

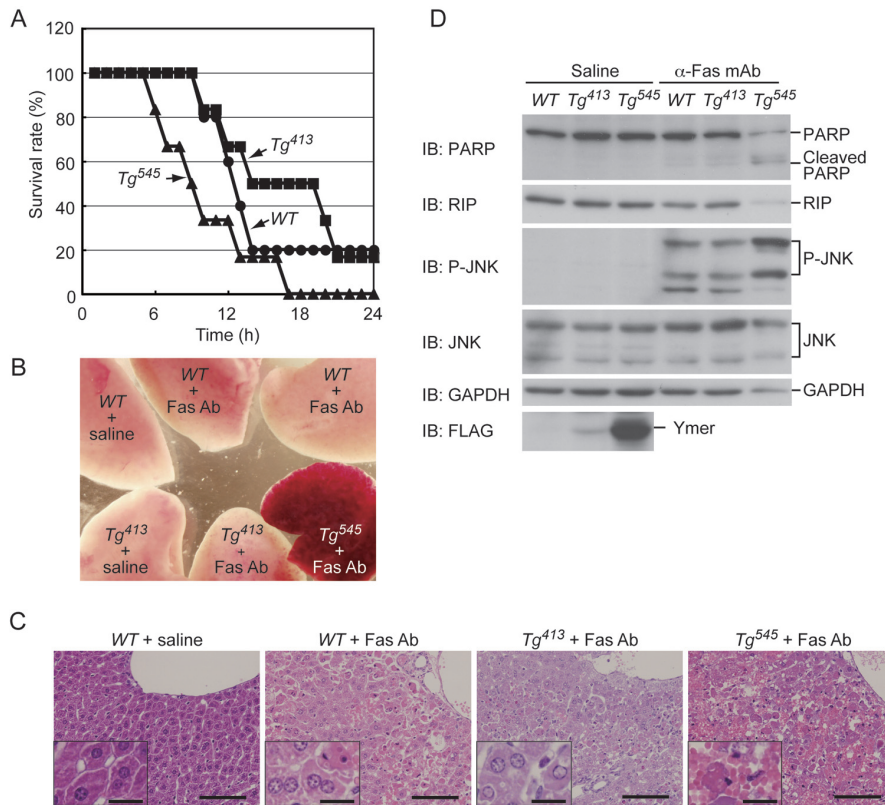


Figure 5. Acceleration of Fas-induced apoptosis in livers of *Ymer Tg* mice. (A) Survival study for Fas-induced cell death was performed with anti-Fas Ab (10 μ g/mouse) intraperitoneal injection into *WT* and *Ymer Tg* mice (*WT*, n = 5; *Tg*⁴¹³, n = 6; *Tg*⁵⁴⁵, n = 6). Survival of the mice was observed for 24 h after injection. Statistical analysis was performed by using the Kaplan-Meier test. (B) Livers treated with anti-Fas Ab were dissected out at 6 h after injection. (C) Livers treated with anti-Fas Ab were dissected out at 4 h after injection and used for histological analysis with HE staining. Scale bars indicate 100 μ m in low magnification and 20 μ m in high magnification (boxed). (D) Immunoblot analysis of apoptosis-related proteins in anti-Fas Ab-treated livers from *Ymer Tg* mice. Two hours after injection with anti-Fas Ab, cell lysates from livers were probed with the indicated Abs.

Ab treatment. Only a slight increase in cleaved products was observed in *WT* and *Tg*⁴¹³ mice, suggesting that *Tg*⁵⁴⁵ mice are sensitive to Fas-mediated apoptosis (Figure 5D) (10). However, these results were not consistent with results presented in Figure 2A, showing TNF α - and LPS-induced cell death, suggesting that the function of Ymer in Fas signaling is different from that in TNFR or TLR4. To clarify the effect of Ymer on Fas-mediated apoptosis, we also tested caspase-independent apoptotic signaling through RIP or JNK. Immunoblot analysis showed reduction of RIP in *Ymer Tg*⁵⁴⁵ mice (Figure 5D). It has been re-

ported that caspase 8 and caspase 10 bind to and cleave RIP (19). These findings indicate that overexpression of Ymer causes activation of caspase-mediated apoptotic cascades in hepatocytes by anti-Fas Ab treatment. Immunoblot analysis showed that JNK in *Ymer Tg*⁵⁴⁵ mice was activated more than that in *WT* or *Tg*⁴¹³ mice. It is known that Fas-induced JNK activation through the Fas-Daxx-Ask1-JNK pathway leads the Bcl2 phosphorylation and consequently causes apoptosis, suggesting that excessive activation of JNK in *Tg*⁵⁴⁵ mice may reduce the antiapoptotic activity of Bcl2 (20,21). Taken together, these results indi-

cate that abundant expression of Ymer may enhance sensitivity to Fas-mediated apoptosis in the liver via caspase and JNK activation.

Ymer Maintains Long-Term Activation of NF- κ B Signaling in Thymocytes

We showed that Ymer accelerates apoptotic cell death and that JNK is activated after Fas stimulation in hepatocytes from *Ymer Tg* mice (Figure 5). It was previously reported that NF- κ B signaling is required for survival of hepatocytes (22–24). Considering these findings, we hypothesized that attenuation of NF- κ B signaling activity by Ymer causes acceleration of Fas-mediated hepatocyte apoptosis in *Ymer Tg* mice. To confirm this hypothesis, we examined Fas-mediated activation of NF- κ B signaling in thymocytes of *WT* and *Ymer Tg*⁵⁴⁵ mice. Immunoblot analysis showed increased cleavage of PARP in *Ymer Tg*⁵⁴⁵ mice compared with that in *WT* mice with anti-Fas Ab treatment, indicating that thymocytes in *Ymer Tg*⁵⁴⁵ mice are also sensitive to anti-Fas Ab treatment (Figures 6A, B). Transient phosphorylation of IKK α / β was observed between 10 and 40 min and was then attenuated after 160 min in *WT* mice. However, phosphorylation of IKK α / β was maintained for a long time (>160 min) in *Ymer Tg*⁵⁴⁵ mice (Figure 6C). Immunoblot analysis showed that the phosphorylation level of IKK α / β in *Ymer Tg*⁵⁴⁵ mice was already higher than that in *WT* mice in a resting state and that IKK α / β was quickly and robustly activated in *Ymer Tg*⁵⁴⁵ mice after Fas stimulation. These findings indicate that attenuation of NF- κ B signaling activity is not the reason for acceleration of Fas-mediated apoptosis in *Ymer Tg* mice and that Ymer may directly affect Fas-mediated apoptotic signal pathways.

DISCUSSION

In this study, to clarify the physiological function of Ymer, we established transgenic mouse strains expressing Ymer. *Ymer Tg* mice showed attenuated activation of NF- κ B signaling in response

to TNF α , polyI:C and LPS stimulation, similar to results of *in vitro* experiments showing that Ymer enhances RIP degradation with A20, followed by suppression of NF- κ B signaling. This study also showed that abundant Ymer expression enhances Fas-mediated JNK phosphorylation and LPS- and polyI:C-induced IFN production and prolongs Fas-induced IKK activation. These findings are in contrast to the results obtained by TNF α -, polyI:C- or LPS-induced NF- κ B activation. Ymer may serve as an activator for the Fas-mediated signaling pathway, whereas it functions as a negative regulator for the TNF α - or LPS-mediated signaling pathway (Figure 6D). Hence, it is important to clarify how Ymer functions as a multifunctional signal regulator downstream of different receptors.

It has been reported that endocytosis of receptors is important to regulate signal activation and that low-temperature treatment of HeLa cells suppressed internalization of TNFR, resulting in inhibition of NF- κ B signaling (25). In addition to this report, monodansylcadaverin, a transglutaminase inhibitor, was shown to prevent endocytosis and suppress TNF α -dependent cell death in U937 cells (26). Others have reported that cytoplasmic translocation of the assembled signaling complex from the cell surface is required for activation of cytokine receptor signaling (27). These findings suggest that internalization of TNFR after TNF α binding is required for the activation of signals including NF- κ B signaling. Furthermore, internalization of Fas or TNFR causes activation of the caspase cascade and sequentially apoptotic cell death (28–30). Taken together, the results suggest that Ymer functions as a general regulator for receptor internalization and that impaired endocytosis of receptors by abundant Ymer expression causes inhibition of NF- κ B signaling via TNFR and TLR4 and causes activation of NF- κ B and JNK via Fas signaling.

It was reported that Ymer interacts with epidermal growth factor receptor (EGFR) to downregulate the receptor localization on the cell surface, suggesting

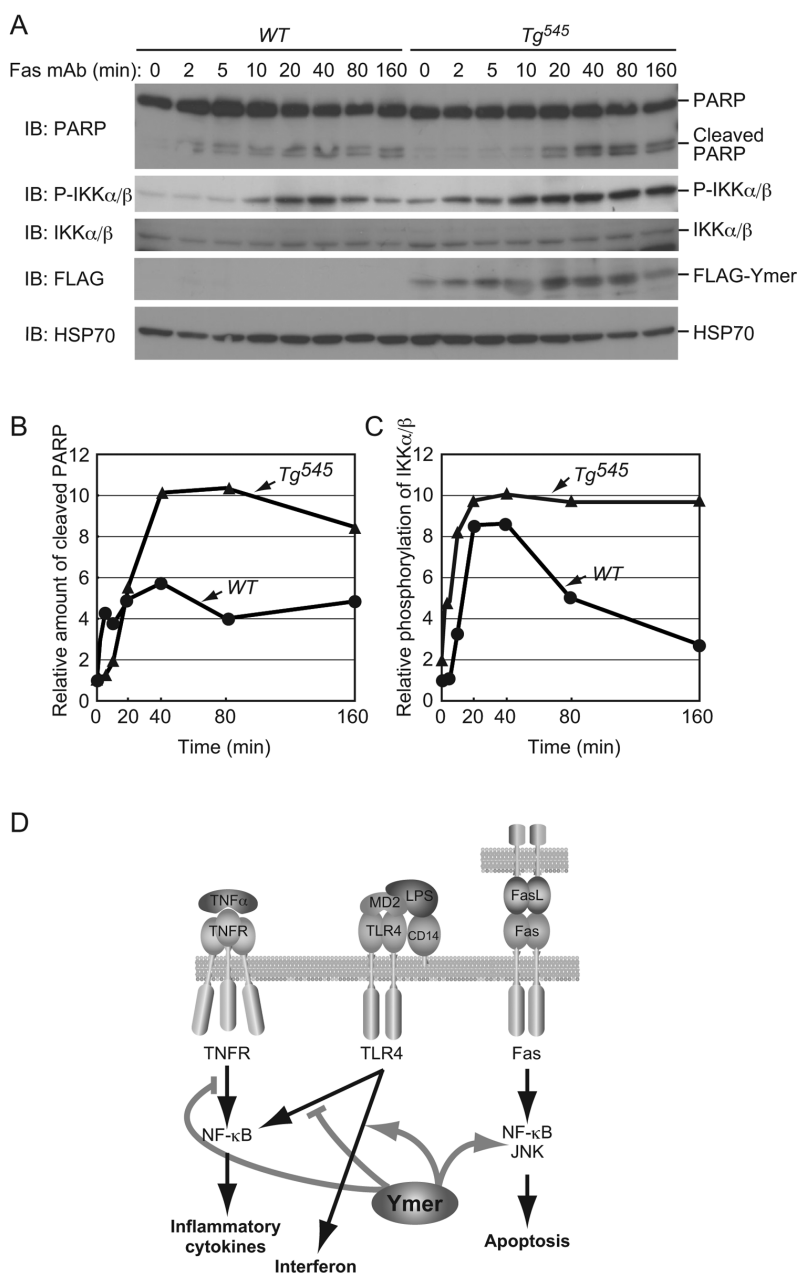


Figure 6. Ymer accelerates the caspase-dependent signal and maintains long-term activation of NF- κ B signaling in Fas-stimulated thymocytes. (A) Thymocytes isolated from WT and *Ymer*⁵⁴⁵ Tg mice were stimulated with anti-Fas Ab (10 μ g/mL) and then probed with the indicated Abs to detect the activation of downstream signaling after stimulation. (B) Time course of cleaved form of PARP in thymocytes from WT and *Ymer*⁵⁴⁵ Tg mice after anti-Fas Ab treatment. A relative amount of the cleaved form of PARP at each time in (A) is shown. The value of the chase period at 0 h was defined as 1. (C) Time course of phosphorylated IKK α / β in thymocytes from WT and *Ymer*⁵⁴⁵ Tg mice after anti-Fas Ab treatment. Relative amount of phosphorylated IKK α / β at each time in (A) is shown. The value of the chase period at 0 h was defined as 1. (D) Model for biological roles of Ymer. Ymer may have multifunctions for several signaling pathways including TLR4, TNFR and Fas. Ymer attenuates NF- κ B signaling downstream of TLR4 and TNFR, whereas it accelerates LPS-induced IFN production and Fas-induced NF- κ B and JNK activation for apoptotic cell death.

that Ymer inhibits internalization and degradation of EGFR after EGF stimulation (31). It was also reported that an E3 ubiquitin ligase, Cbl, ubiquitinates the cytoplasmic domain of EGFR in a phosphorylation-dependent manner and regulates EGFR internalization (32,33) and that E2 ubiquitin-conjugating enzymes Ubc4/5 and Cbl have the ability to conjugate the K63-linked polyubiquitin chain, suggesting that the K63-linked polyubiquitin chain regulates internalization of EGFR (34–36). Moreover, we showed that Ymer selectively interacts with K63-linked polyubiquitin (6). Taken together, the results suggest that Ymer likely regulates internalization of receptors via K63-linked ubiquitination for EGFR, TNFR, TLR4 and Fas. However, flowcytometric analysis using an antibody to each receptor showed that there was no difference in receptor internalization of TLR4, TNFR or Fas between *Ymer Tg* and *WT* mice, suggesting that Ymer does not affect receptor internalization and internalization-dependent switching of signaling pathways (Supplementary Figure 5). These findings suggest that Ymer functions at a stage downstream of receptor internalization after stimulus and upstream of IKK α / β activation.

We showed that activation of NF- κ B is inhibited in *Ymer Tg* mice, whereas IFN expression is induced by LPS in *Ymer Tg* mice. It was reported that LPS-induced activation of macrophages is regulated by two different signaling mechanisms: one is Myd88-dependent NF- κ B and MAPK activation and the other is TRIF-dependent IFN induction via TANK-binding kinase (TBK)/IKK ϵ and interferon regulatory factor 3 (IRF3) (37–39). We examined whether Ymer overexpression affects polyI:C-induced IFN α expression through TLR3, which does not recruit MyD88 but depends solely on TRIF. Our results showed that IFN α induction was enhanced in *Ymer Tg* mice with polyI:C stimulation, suggesting that Ymer affects the TRIF-dependent pathway via a mechanism different from that in Myd88-dependent signaling.

It is important to clarify how Ymer accelerates IKK activation and JNK phosphorylation via Fas-mediated signaling. Our results indicate that Ymer may have reciprocal roles between TNFR and Fas. It was reported that Fas signaling involves RIP to activate NF- κ B and that RIP is independent of Fas-mediated signaling (40,41). Therefore, although Ymer interacts and inhibits the function of RIP, it is not clear whether Ymer affects Fas-mediated signals via modulation of RIP.

CONCLUSION

In summary, our results indicate that Ymer is a novel multifunctional signal regulator in several signaling pathways for inflammation, cell death and proliferation. It is important to determine the functions of Ymer and the binding partners to Ymer in each signaling pathway in the future. Therefore, a genetic approach using knockout mice is needed to clarify physiological functions of Ymer. Further analysis of Ymer may prove to provide therapeutic benefits not only for the suppression in inflammation and autoimmune diseases but also for the inhibition of growth of cancer cells.

ACKNOWLEDGMENTS

We thank Jun Miyazaki for the plasmids, Akihiro Ishizu for histological analysis and Yuri Soida for helping prepare the manuscript.

This work was supported in part by KAKENHI from the Ministry of Education, Culture, Sports, Science and Technology (18076001, 21390087 to S Hatakeyama).

DISCLOSURE

The authors declare that they have no competing interests as defined by *Molecular Medicine*, or other interests that might be perceived to influence the results and discussion reported in this paper.

REFERENCES

- Hayden MS, Ghosh S. (2004) Signaling to NF- κ B. *Genes. Dev.* 18:2195–224.
- Yaron A, et al. (1998) Identification of the receptor component of the IkappaBalpha-ubiquitin ligase. *Nature.* 396:590–4.

- Hatakeyama S, et al. (1999) Ubiquitin-dependent degradation of IkappaBalpha is mediated by a ubiquitin ligase Skp1/Cul 1/F-box protein FWD1. *Proc. Natl. Acad. Sci. U. S. A.* 96:3859–63.
- Lee EG, et al. (2000) Failure to regulate TNF-induced NF-kappaB and cell death responses in A20-deficient mice. *Science.* 289:2350–4.
- Wertz IE, et al. (2004) De-ubiquitination and ubiquitin ligase domains of A20 downregulate NF-kappaB signalling. *Nature.* 430:694–9.
- Bohgaki M, et al. (2008) Involvement of Ymer in suppression of NF-kappaB activation by regulated interaction with lysine-63-linked polyubiquitin chain. *Biochim. Biophys. Acta.* 1783:826–37.
- Niwa H, Yamamura K, Miyazaki J. (1991) Efficient selection for high-expression transfectants with a novel eukaryotic vector. *Gene* 108:193–9.
- Committee for the Update of the Guide for the Care and Use of Laboratory Animals, Institute for Laboratory Animal Research, Division on Earth and Life Studies, National Research Council of the National Academies. (2011) *Guide for the Care and Use of Laboratory Animals*. 8th edition. Washington (DC): National Academies Press. [2012 Jun 1]. Available from: <http://oacu.od.nih.gov/regs/>
- Matsuda M, Tsukiyama T, Bohgaki M, Nonomura K, Hatakeyama S. (2007) Establishment of a newly improved detection system for NF-kappaB activity. *Immunol. Lett.* 109:175–81.
- Lazebnik YA, Kaufmann SH, Desnoyers S, Poirier GG, Earnshaw WC. (1994) Cleavage of poly(ADP-ribose) polymerase by a proteinase with properties like ICE. *Nature* 371:346–7.
- Wullaert A, van Loo G, Heyninck K, Beyaert R. (2007) Hepatic tumor necrosis factor signaling and nuclear factor-kappaB: effects on liver homeostasis and beyond. *Endocr. Rev.* 28:365–86.
- Casiano CA, Ochs RL, Tan EM. (1998) Distinct cleavage products of nuclear proteins in apoptosis and necrosis revealed by autoantibody probes. *Cell Death Differ.* 5:183–90.
- Salgado A, et al. (1994) Inflammatory mediators and their influence on haemostasis. *Haemostasis.* 24:132–8.
- Morikawa A, et al. (2000) Augmentation of nitric oxide production by gamma interferon in a mouse vascular endothelial cell line and its modulation by tumor necrosis factor alpha and lipopolysaccharide. *Infect. Immun.* 68:6209–14.
- Moynagh PN. (2005) TLR signalling and activation of IRFs: revisiting old friends from the NF-kappaB pathway. *Trends Immunol.* 26:469–76.
- Gauzzi MC, Del Corno M, Gessani S. (2010) Dissecting TLR3 signalling in dendritic cells. *Immunobiology.* 215:713–23.
- Kelley VE, Roths JB. (1985) Interaction of mutant *lpr* gene with background strain influences renal disease. *Clin. Immunol. Immunopathol.* 37:220–9.
- Holler N, et al. (2000) Fas triggers an alternative, caspase-8-independent cell death pathway using the kinase RIP as effector molecule. *Nat. Immunol.* 1:489–95.
- Fischer U, Stroh C, Schulze-Osthoff K. (2006)

- Unique and overlapping substrate specificities of caspase-8 and caspase-10. *Oncogene*. 25:152–9.
20. Chang HY, Nishitoh H, Yang X, Ichijo H, Baltimore D. (1998) Activation of apoptosis signal-regulating kinase 1 (ASK1) by the adapter protein Daxx. *Science*. 281:1860–3.
 21. Yamamoto K, Ichijo H, Korsmeyer SJ. (1999) BCL-2 is phosphorylated and inactivated by an ASK1/Jun N-terminal protein kinase pathway normally activated at G(2)/M. *Mol. Cell. Biol.* 19:8469–78.
 22. Beg AA, Sha WC, Bronson RT, Ghosh S, Baltimore D. (1995) Embryonic lethality and liver degeneration in mice lacking the RelA component of NF-kappa B. *Nature*. 376:167–70.
 23. Weih F, et al. (1997) p50-NF-kappaB complexes partially compensate for the absence of RelB: severely increased pathology in p50(-/-)relB(-/-) double-knockout mice. *J. Exp. Med.* 185:1359–70.
 24. Li Q, Van Antwerp D, Mercurio F, Lee KF, Verma IM. (1999) Severe liver degeneration in mice lacking the IkappaB kinase 2 gene. *Science*. 284:321–5.
 25. Andrieu N, Salvayre R, Jaffrezou JP, Levade T. (1995) Low temperatures and hypertonicity do not block cytokine-induced stimulation of the sphingomyelin pathway but inhibit nuclear factor-kappa B activation. *J. Biol. Chem.* 270:24518–24.
 26. Schutze S, et al. (1999) Inhibition of receptor internalization by monodansylcadaverine selectively blocks p55 tumor necrosis factor receptor death domain signaling. *J. Biol. Chem.* 274:10203–12.
 27. Matsuzawa A, et al. (2008) Essential cytoplasmic translocation of a cytokine receptor-assembled signaling complex. *Science*. 321:663–8.
 28. Micheau O, Tschopp J. (2003) Induction of TNF receptor I-mediated apoptosis via two sequential signaling complexes. *Cell*. 114:181–90.
 29. Lee KH, et al. (2006) The role of receptor internalization in CD95 signaling. *EMBO J.* 25:1009–23.
 30. Schutze S, Tchikov V, Schneider-Brachert W. (2008) Regulation of TNFR1 and CD95 signalling by receptor compartmentalization. *Nat. Rev. Mol. Cell Biol.* 9:655–62.
 31. Tashiro K, et al. (2006) Suppression of the ligand-mediated down-regulation of epidermal growth factor receptor by Ymer, a novel tyrosine-phosphorylated and ubiquitinated protein. *J. Biol. Chem.* 281:24612–22.
 32. Levkowitz G, et al. (1999) Ubiquitin ligase activity and tyrosine phosphorylation underlie suppression of growth factor signaling by c-Cbl/Sli-1. *Mol. Cell*. 4:1029–40.
 33. Yokouchi M, et al. (1999) Ligand-induced ubiquitination of the epidermal growth factor receptor involves the interaction of the c-Cbl RING finger and UbcH7. *J. Biol. Chem.* 274:31707–12.
 34. Umebayashi K, Stenmark H, Yoshimori T. (2008) Ubc4/5 and c-Cbl continue to ubiquitinate EGF receptor after internalization to facilitate polyubiquitination and degradation. *Mol. Biol. Cell*. 19:3454–62.
 35. Xu M, Skaug B, Zeng W, Chen ZJ. (2009) A ubiquitin replacement strategy in human cells reveals distinct mechanisms of IKK activation by TNF alpha and IL-1beta. *Mol. Cell*. 36:302–14.
 36. Zeng W, Xu M, Liu S, Sun L, Chen ZJ. (2009) Key role of Ubc5 and lysine-63 polyubiquitination in viral activation of IRF3. *Mol. Cell*. 36:315–25.
 37. Kawai T, Adachi O, Ogawa T, Takeda K, Akira S. (1999) Unresponsiveness of MyD88-deficient mice to endotoxin. *Immunity*. 11:115–22.
 38. Yamamoto M, et al. (2003) Role of adaptor TRIF in the MyD88-independent toll-like receptor signaling pathway. *Science*. 301:640–3.
 39. Dauphinee SM, Karsan A. (2006) Lipopolysaccharide signaling in endothelial cells. *Lab. Invest.* 86:9–22.
 40. Kreuz S, et al. (2004) NFkappaB activation by Fas is mediated through FADD, caspase-8, and RIP and is inhibited by FLIP. *J. Cell Biol.* 166:369–80.
 41. Villunger A, Huang DC, Holler N, Tschopp J, Strasser A. (2000) Fas ligand-induced c-Jun kinase activation in lymphoid cells requires extensive receptor aggregation but is independent of DAXX, and Fas-mediated cell death does not involve DAXX, RIP, or RAIDD. *J. Immunol.* 165:1337–43.